A Retrospective Study of Commercial Software System EDose in QA Application based on the Electronic Portal Imaging Device

Xiaojuan Duan
Third Military Medical University Second Affiliated Hospital: Xinqiao Hospital
Hongya Dai
Third Military Medical University Second Affiliated Hospital: Xinqiao Hospital
Yongqin Li
3rd Military Medical University: Army Medical University
Yibing Zhou (xqrt2020@163.com)
Third Military Medical University Second Affiliated Hospital: Xinqiao Hospital

Research Article

Keywords: EDose, EPID, Seven29, 3Dmap, Action level, 3D online, Dose verification

Posted Date: September 30th, 2021

DOI: https://doi.org/10.21203/rs.3.rs-683325/v1

Abstract

Purpose: To evaluate the functions about the pre-treatment dose verification and, the in vivo dose verification for the commercial software EDose system based on Electronic Portal Imaging Device (EPID) retrospectively and establish the action limit level.

Methods: The results of pre-treatment dose verification were compared with 2D array Seven29 and 3Dmap for 50 randomly selected IMRT plans of different lesions. A retrospective analysis was conducted for 287 radiotherapy plans using the EDose in pre-treatment dose verification, including 53 IMRT and 247 RapidArc plans, to establish the action limit level with statistical significance evaluation. 28 head and neck patients with different lesions were selected randomly for studying 3D online dose verification preliminary.

Results: For pre-treatment dose verification, 50 plans' average γ passing rates of the 3%/3mm criterion were > 98% for EDose, Seven29, 3Dmap, and 3%/2mm, 2%/2mm criteria were > 95%, 90%. The average γ_{mean} of the three verification methods were similar for the 3%/3mm criterion (0.35, 0.38, 0.35). Based on the 287 patients' clinical data, the average γ passing rate was 97.5%, and the recommend clinical action level was established at 92% with a 95% confidence limit. The in vivo results showed that the γ pass rate had a decreasing trend as the 33 treatment fractions progressed. The γ passing rates means±SD of the first fraction was (91.92±3.31)% while the 33th fraction was (85.73±8.75)%. In addition, the standard deviation between the TPS calculations and the EDose measurement results indicated a higher value of the thirty-third treatment for PTVs and organ at risk compared to the first treatment.

Conclusions: This study demonstrated that the EDose system is an accurate, efficient method for quality assurance of patient' radiotherapy plans with remarkable consistency of treatment planning system (TPS).

Introduction

Radiotherapy experienced a fundamental change in approach by transiting from conventional two-dimensional radiotherapy (2DRT) to three-dimensional conformal radiotherapy (3DCRT) in the last two decades. The technique of small fields shaped by multileaf collimators (MLCs) makes the 3DCRT more complicated, while tight margins became the general practice. Numerous complex treatment plans became available with the implementation of intensity modulated radiotherapy (IMRT) and volumetric modulated arc therapy (RapidArc), as well as with the clinical use of proton and carbon ion beams.[1] Quality assurance (QA) is required for ensuring the accuracy of these complex treatment plans, as discussed in many reports.

The film has a long and extensive use to validate the planar dose in radiotherapy. However, film processing is logging, time-consuming, and dosimetry uncertainty may be brought for its calibration curve.[2] 2D and 3D detectors have become the standard device for QA measurement in modern radiotherapy for the characteristics of convenience, accuracy, and efficiency.[3] These multidimensional detectors have adequately characterized for clinical use. However, when superior spatial resolution is required, radiochromic films are often the preferred method. EPID has been used as a preferred tool to verify the patient positioning undergoing radiotherapy in recent decades. The application of QA measurement has been investigated due to the favorable characteristics of the amorphous silicon EPID such as fast image acquisition, high resolution, digital format, in vivo measurement.[4]

Current, commercially available a-Si EPID systems were discussed, highlighting dosimetric characteristics and technical challenges to routine use. Our radiotherapy center implemented the commercial software product EDose using EPID in 2018, which had become an option of large-scale patient IMRT and RapidArc dose verification. This study aims to investigate the dosimetric characteristics of the EDose system, discuss the feasibility in pre-treatment verification, the application in 3D online dose verification, and establish clinical action levels.

Materials And Methods

Measuring systems

A Varian trilogy linear (Varian Medical System, Palo Alto, CA) with a 6MV photon beam had been used in this study. The accelerator is equipped with a standard MLC that consists of two leaf banks of 40 leaves each, 1 cm wide at the isocenter distance of 100 cm, and the IMRT delivery is performed with a sliding window technique. The Varian aSi1000 EPID has an area of 40×32cm^2 with a pixel dimension of 1024×768, a spatial resolution of 0.392mm per pixel, and no angular response. EPID consists of several layers, and the measured aSi image is converted to dose to water at a certain depth in the uniform water equivalent phantom.

The software EDose system is an EPID-based three-dimensional dose monitoring system for intensity-modulated radiation therapy. It mainly consists of three-dimensional dose reconstruction and analysis. The software system EDose basing on the patients' anatomy, uses the image pixel values captured by EPID in the air without a phantom/patient as the input parameters and reconstructs into a fluence map of the delivered beam through deconvolution and convolution. The system consists of three functional modules: 1. independent checking of the treatment plan; 2. 3D dosimetric verification before treatment; 3. Real-time 3D online monitoring dose during treatment. Dose calculation and gamma evaluation adopt the collapsed cone convolution superposition (CCCS) algorithm.

The workflow of EDose system is shown in Fig. 1. Firstly, the fluence map is derived from the EPID measurement results based on the patient or model. Then, the GPU-based CCC algorithm is used to carry out 3D dose reconstruction on Planning CT. Finally, the three-dimensional dose reconstructed by the EDose system is compared with the calculated results of TPS. The fluence maps were reconstructed from the EPID image according to the theoretical formulas[,] as follow:

$$D_{ij} = c_{ad} \cdot P_{ij} \otimes^{-1} K_1(d_{ij}) \otimes K_2(d_{ij}) \quad (1)$$

where

$$K_1(d_{ij}) = (1-c)e^{-\mu_1 d_{ij}} + ce^{-\mu_2 d_{ij}} \quad (2)$$

$$K_2(d_{ij}) = \mathrm{e}^{-\mu_3 \mathrm{d_{ij}}} \quad (3)$$

where "D_{ij}" is the dose at the phantom level, "C_{ad}" is the absolute dose calibration factor, "P_{ij}" is the EPID image pixel values, "d_{ij}" is the distance from the center of the kernel to a pixel ij, "$K1(d_{ij})$" is the scattering kernel of the EPID and $K2(d_{ij})$ is the fuzzy convolution kernel, "$\otimes$" and "$\otimes^{-1}$ " represent the convolution and deconvolution operators, respectively. What's more, μ_1 and μ_2 are the attenuation coefficients, μ_3 affects the gradient of the penumbra, c is the ratio constant.

The automatic evaluation tools included the three-dimensional isodose distribution, the three-dimensional gamma analysis, the dose profile distribution, and the detailed dose-volume histogram analysis of the target area and organs at risk, illustrated in Fig. 2.

The 2D-array Seven29 (Physikalisch Technische Werkstatten, Freiburg, Germany) is equipped with 729 vented plane parallel ion-chambers over an area of 27×27cm^2. The Seven29 utilizes 5×5mm^2 cross-sectional chambers with a 0.6g/cm^2 graphite wall, 5 mm air-filled height, spaced 1cm apart. The linearity is less than 0.4% from doses of 2 ~ 500MU. The short-term and long-term (4 months) reproducibility is found to be 0.2% and 1%, respectively.[,] Typically, additional solid water slabs were placed so that the effective measurement plane was in the depth 5 cm and the backscattering thickness of 5cm.

The two-dimension array 3Dmap (Raydose Medical Technology, Guangzhou, China) is similar to a mobilizable EPID, which detector is amorphous silicon and has a spatial resolution of 0.14mm per pixel with an array of 2048×2048 pixels and a field

size of 28.6×28.6cm^2. The dose linearity and reproducibility are both 0.5%.

Feasibility of EDose in pre-treatment verification

EDose had been introduced in our department in August 2018 based on the Varian aSi1000 EPID. We randomly selected 50 IMRT/RapidArc plans optimized by the Varian Eclipse TPS (version 8.6), nasopharyngeal, glioblastoma, cerebral metastatic, parotid gland, and larynx carcinoma, for pre-treatment verification by three methods EDose, seven29, 3Dmap separately to verify the feasibility of the EDose system. The panel of EPID detectors was positioned at the isocenter with a distance of 100cm without any attenuating material in between (Fig. 2(a)). Gamma analysis with percent dose acceptance criteria and distance to agreement criteria of 3%/3mm, 3%/2mm, and 2%/2mm passing criteria under a dose threshold of 10% of the maximum dose on each plane were used.

Clinical action level

A retrospective analysis was performed for 287 radiotherapy plans using the EDose in pre-treatment dose verification, including 53 IMRT and 247 RapidArc plans. According to the disease anatomy sites, the treatment plans were divided into Brain 102, Head & Neck 138, Abdomen 11, Pelvis 20, Bone 23, and other disease sites 6. The gamma passing rates with criteria 3%/3mm, 3%/2mm, and 2%/2mm also were analyzed statistically.

TG119 used the concept of “confidence limit” to describe how closely the set of measurements agreed with the planned values. The confidence limit was defined as CL= (100-mean) + 1.96σ, where mean and σ were the institutional mean percentage of points passing the gamma criteria and the standard deviation. The clinical action levels were established according to the TG-119 reports’ suggestion: For a large number of gamma analyses, 95% of the tests should result in pass rates that exceed (100-CL)%.[]

3D online (in vivo) verification

28 randomly patients with head and neck lesions (17 nasopharyngeal carcinoma, 11 laryngeal cancer) were selected for conducting 3D online dose verification preliminary. The panel of EPID detectors was positioned at a distance of 150cm with the patient in between (Fig. 2(b)).

Result

Feasibility of EDose for pre-treatment dose verification

A γ value of 1.0 or less indicates that a particular point falls within the criteria of 3% dose difference and 3mm DTA and, therefore, is a passing point. The γ passing rates obtained from the EDose, Seven29, and 3Dmap were compared with the TPS calculations. The average (avg.), minimum (min.), maximum (max.), and standard deviation (SD) of the γ passing rates and γ_{mean} of 50 selected cases for the criteria 3%/3mm, 3%/2mm, and 2%/2mm were shown in Table 1.

All plans’ average γ passing rates of the 3%/3mm criterion was > 98% for EDose, Seven29, and 3Dmap. The corresponding average γ passing rates when using criteria of 3%/2mm and 2%/2mm were > 95% and 90%. So, all plans were acceptable according to AAPM Task Group 119 that the planar dose distributions were assessed using gamma criterion of 3%/3 mm. Additionally, The average γ_{mean} of the three dose verification methods were similar for the 3%/3mm (0.35, 0.38, 0.35), 3%/2mm (0.41, 0.48, 0.43) and 2%/2mm criteria (0.50, 0.56, 0.55).

The SD of γ passing rates of the 3%/3mm criterion was 1.69%, 1.61%, 1.37% for EDose, Seven29, 3Dmap severally, and the corresponding the 3%/2mm criterion was 2.89%, 3.04%, 2.17%. Therefore, the narrow range of SD showed the fine reproducibility and stability of the response obtained using the EDose system, and consistent with the other two methods.

Table 1
Overview of avg., min., max., and SD value of γ passing rates and γ_{mean} obtained using EDose, Seven29 and 3Dmap for 50 cases.

		3%/3mm			3%/2mm			2%/2mm		
		EDose	Seven29	3Dmap	EDose	Seven29	3Dmap	EDose	Seven29	3Dmap
γ passing rate	avg. [%]	98.12	98.35	98.53	95.53	96.53	95.41	91.59	94.69	90.90
	min. [%]	93.32	93.60	93.98	88.61	87.20	88.55	74.04	82.50	78.25
	max. [%]	99.85	100.00	100.00	99.17	100.00	98.38	98.38	100.00	96.69
	SD [%]	1.69	1.61	1.37	2.89	3.04	2.17	5.53	3.76	3.81
γ_{mean}	avg.	0.35	0.38	0.35	0.41	0.48	0.43	0.50	0.56	0.55
	min.	0.25	0.27	0.23	0.29	0.29	0.30	0.35	0.40	0.38
	max.	0.57	0.56	0.45	0.69	0.72	0.58	0.81	0.87	0.73
	SD	0.07	0.07	0.05	0.08	0.09	0.06	0.10	0.10	0.08

Small differences were observed in γ passing rates and γ_{mean} when comparing the three dose verification methods (EDose, Seven, and 3Dmap) for all the selected cases. Obtained average γ passing rates were similar with 98.12%, 98.35%, 98.53% for EDose, Seven, 3Dmap respectively to 3%/3mm criterion, and corresponding 95.53%, 96.53%, 95.54–3%/2mm criterion. However, Seven 29 exhibited higher average γ passing rates (94.69%) compared to EDose (91.59%) and 3Dmap (90.90%) to 2%/2mm criterion.

The γ passing rates and γ_{mean} for the 5 kinds of disease obtained from EDose, Seven29, and 3Dmap were shown in Fig. 3 and Fig. 4. We could see the average γ passing rates of the larynx cancer were consistent among the three dose verification methods for three passing rates criteria (3%/3mm, 3%/2mm, 2%/2mm). For the 3%/3mm criterion, the average γ passing rates was acceptable in all the nasopharyngeal, glioblastoma, cerebral metastatic, parotid gland, and larynx cancer groups, with an average rates of (96.60 ± 2.17)%, (98.83 ± 1.77)%, (98.85 ± 1.05)%, (98.12 ± 1.24)%, (98.20 ± 1.18)% for EDose, (97.43 ± 1.37)%, (98.03 ± 1.48)%, (98.87 ± 1.33)%, (99.18 ± 1.35)%, (98.22 ± 2.07)% for Seven29, and (98.32 ± 1.14)%, (98.63 ± 1.24)%, (98.44 ± 1.85)%, (98.32 ± 1.37)%, (98.92 ± 1.32)% for 3Dmap, respectively.

The differences among the three methods gradually increased with increasing the criteria from 3%/3mm to 3%/2mm to 2%/2mm, shown in Fig. 5. The maximum difference (4.49%) of the γ passing rate was found in the nasopharyngeal cancer (NPC) group at the 2%/2mm criterion, while the differences of the other four groups were both < 3%, and the larynx cancer was only 0.88%. The corresponding differences at 3%/2mm, 3%/3mm criteria were < 2%, 1% separately and the larynx cancer was < 0.5%.

Fig. 4γ passing rates for the 5 kinds of disease obtained from EDose,Seven29 and 3Dmap measurements respectively. (a) 3%/3mm criteria; (b) 3%/2mm criteria; (c) 2%/2mm criteria; The columns represent the mean values of the γ passing rates, and the error bars are the correspondingSD.

Fig. 5 γ_{mean} for the 5 kinds of disease obtained from EDose,Seven29 and 3Dmap measurements respectively. (a) 3%/3mm criteria; (b) 3%/2mm criteria; (c) 2%/2mm criteria; The columns represent the mean values of the γ_{mean} and the error bars are the correspondingSD.

Action level

With a total of 287 clinical patients' plans verified by EDose, the γ passing rates were summarized with various disease sites under the three criteria 3%/3mm, 3%/2mm, and 2%/2mm, illustrated in Table 2 and Fig. 6. We set action levels for our clinic using the gamma values calculated. Specifically, we established a set of action levels based on the institutional average values and standard deviations.

The percentage of points passing the 3%/3mm criterion was on average (98.11 ± 2.05)% for brain case, (97.34 ± 2.20)% for H&N case, (98.10 ± 2.97)% for the abdomen, (95.59 ± 2.59)% for pelvis case, (96.53 ± 2.33)% for the bone case, and (97.79 ± 1.23)% for other cases. The overall results were (97.46 ± 2.31)%. Thus, the corresponding action level was 93%, according to the definition described in TG-119 reports. The average percentage of points passing the criteria of 3%/2mm and 2%/2mm were (94.87 ± 3.78)% and (89.29 ± 7.49)%, well the corresponding action levels of 87% and 75%, respectively.

Table 2
γ passing rates of 287 cases with EDose method for 3%/3mm, 3%/2mm, and 2%/2mm criteria in different disease sites.

sites	number of cases	3%/3mm [%]		3%/2mm [%]		2%/2mm [%]	
		avg.±SD	range	avg.±SD	range	avg.±SD	range
Brain	102	98.11 ± 2.05	92.45–99.96	95.8 ± 3.74	82.65–99.44	90.20 ± 8.14	68.09–98.80
H&N	127	97.34 ± 2.20	90.85–99.84	94.42 ± 3.69	83.80–99.11	89.15 ± 7.00	68.83–98.28
Abdomen	10	98.10 ± 2.97	91.16–99.92	96.52 ± 4.52	86.37–99.66	91.07 ± 10.37	71.64–99.15
Pelvis	19	95.59 ± 2.59	91.34–99.99	92.80 ± 3.83	86.19–99.93	84.82 ± 6.62	73.74–99.22
Bone	23	96.53 ± 2.33	91.82–99.74	94.06 ± 3.35	84.93–99.20	88.60 ± 5.33	76.56–97.70
Other	6	97.79 ± 1.23	96.08–99.06	95.61 ± 2.10	92.47–98.10	91.12 ± 5.68	80.75–95.70
Total	287	97.46 ± 2.31	90.85–99.99	94.87 ± 3.78	82.65–99.93	89.29 ± 7.49	68.09–99.22

3D online (in vivo) verification

28 randomly head and neck patients including 17 nasopharyngeal carcinomas, six laryngeal cancer, five oropharyngeal cancer) had been selected for conducting 3D in vivo dose verification at each treatment fraction. The average γ pass rate under the 3%/3 mm criterion for all 28 patients was obtained by comparing the 3D dose-reconstruction results from the EDose and the calculation results from the TPS, shown in Fig. 7. The results showed that the in vivo γ pass rate had a decreasing trend during the 33 treatment fractions. The γ passing rates means ± SD of the first fraction was (91.92 ± 3.31)% while the 33th fraction was (85.73 ± 8.75)%. The dotted line was the linear regression of the average γ pass rate and a linear coefficient of determination $y = -0.1624x + 89.49$, $R^2 = 0.1855$.

The difference analysis of the DVH index for the first, the seventh, and the thirty-third were shown in Table3. The comparison results are expressed as the means ± SD for 28 head and neck patients. As illustrated in Table 3,

Compared to the TPS calculations, the average D_{98} of the PTVs obtained using EDose for the first treatment showed that the deviations were less than 3%, except the PGTVnd, which was − 3.72%. While the seventh treatment was more than 3% except the PGTVnx was − 2.63%, and the thirty-third treatment were all less than 3%. The ΔD_{mean} of the PGTVnx, PGTVnd, PCTV1, PCTV2 for the first treatment were (5.94 ± 2.62)%, (0.96 ± 2.04)%, (3.79 ± 2.39)%, (2.26 ± 2.24)%, the seventh treatment were (2.75 ± 3.58)%, (-0.30 ± 3.29)%, (0.72 ± 4.07)%, (-0.47 ± 3.65)% and the thirty-third treatment were (5.51 ± 7.41)%, (2.09 ± 7.54)%, (3.64 ± 6.34)%, (4.89 ± 9.43)%, respectively. The means ΔD_{max} of the PTVs were large for these three treatment stages, all greater than 3%. The similar results were also obtained for organ at risk. The standard deviation (SD) indicated a higher value of the thirty-third for PTVs and organ at risk compared to the first treatment.

Two patient data examples with the maximum difference in passing rate were compared, which the γ image distributions in the transverse view and γ histogram were shown in Fig. 8. Figure (a) was a brain metastasis patient with a γ passing rate of 99.84%, γ_{mean} 0.281, SD 0.188, while figure (b) was a rectal cancer patient with a γ passing rate of 91.70%, γ_{mean} 0.487, SD 0.336. As shown in the γ image, the green represented the passing region, while the pink region represented the failure to pass. We could see that there was some normal tissue outside the planning target volume of rectal cancer were unacceptable results, and γ distribution of rectal cancer was higher and wider than brain metastases from the histogram.

Table 3
DVH comparison between EDose and TPS for the 1st, 17th and the 33rd

Evaluated Organs		PGTVnx	PGTVnd	PCTV1	PCTV2	Brain stem	Spinal cord	Parotid gland L	Parotid gland R
1st	ΔD_{98} [%]	0.27 ± 5.70	-3.72 ± 4.10	-2.24 ± 7.16	-2.92 ± 4.11				
	ΔD_{mean} [%]	5.94 ± 2.62	0.96 ± 2.04	3.79 ± 2.39	2.26 ± 2.24				
	ΔD_{max} [%]	7.85 ± 3.05	4.78 ± 2.50	7.24 ± 2.54	4.92 ± 4.70	9.08 ± 4.82	5.52 ± 4.09		
	ΔD_{50} [%]							2.87 ± 4.98	2.79 ± 4.16
17th	ΔD_{98} [%]	-2.63 ± 5.40	-5.79 ± 4.36	-6.13 ± 8.83	-6.25 ± 2.86				
	ΔD_{mean} [%]	2.75 ± 3.58	-0.30 ± 3.29	0.72 ± 4.07	-0.47 ± 3.65				
	ΔD_{max} [%]	5.01 ± 3.36	3.24 ± 3.23	4.40 ± 3.37	3.24 ± 3.53	5.02 ± 7.74	1.29 ± 5.31		
	ΔD_{50} [%]							-0.84 ± 6.76	0.50 ± 9.95
33th	ΔD_{98} [%]	2.70 ± 8.28	-2.63 ± 8.57	-0.97 ± 9.75	1.18 ± 12.18				
	ΔD_{mean} [%]	5.51 ± 7.41	2.09 ± 7.54	3.64 ± 6.34	4.89 ± 9.43				
	ΔD_{max} [%]	7.79 ± 6.94	5.92 ± 7.86	6.87 ± 6.00	5.31 ± 12.88	8.69 ± 7.14	6.07 ± 8.91		
	ΔD_{50} [%]							6.62 ± 6.86	3.21 ± 15.22

To observe the difference between the 3D online and pre-treatment dose verification, a cervical lymph node metastases plan was adopted as an example, Fig. 9 showed γ image distributions of the 3D online (Fig. 9(a)) and pre-treatment (Fig. 9(b)) dose distributions in isocentric plane of three axes, where the passing rate of 3D online and pre-treatment were 97.06% and 95.60%, γ_{mean} 3D online and pre-treatment were 0.38 and 0.41. The sky blue represented the passing region, while the yellow area represented the failed region. As shown in the pictures, the result distributions were similar between the 3D online and pre-treatment, and the failed areas were mainly distributed in regions of the low dose and areas close to the skin.

Discussion

The investigations have confirmed in the literature that the EPID-based QA using different methods is a powerful tool for dosimetric verification of complex radiotherapy such as IMRT/RapidArc.[8–13,] The EDose system has been used for Linac based IMRT/RapidArc specific QA.[] In the study, the basic functional performance of the EDose system was tested based on Varian aSi1000 EPID. These tests showed excellent dosimetric characteristics justifying the development and use of a universal, optimized dose verification strategy.

As expected, the EDose system demonstrates favorable dosimetric properties, such as excellent accuracy and reproducibility. All results are integrated into the EDose solution. The linearity is smaller than the results obtained from the publication using EPID,[] it presents linearity deviations up to 10% from the theoretically expected value for dose acquisitions of 10 MU, whereas dosimetric images of 1000 MU can be off by 1–2%. Berry et al.[] have proposed the accurate field size dependence algorithms, which present the major advantage that it can be integrated into the existing portal dosimetry solution preserving high efficiency in clinical routine. In our study, concerning field size dependence, the difference between measurements and calculations are found to be within ± 0.7%, except the maximum 0.72% for field sizes 3×3cm2. Field sizes less than 3×3cm2 are considered small fields for 6 MV (International Atomic Energy Agency [IAEA], 2017).[] Small-field dosimetry places stringent requirements on detectors. Not only the dimensions of the detector are important, but also its density, atomic number, and water equivalence all affect the measurements.[1,] So, the discussion on small-field dosimetry is not presented.

In the feasibility study of EDose for pre-treatment dose verification, three detector systems showed good response for IMRT specific QA. All plans' average γ passing rates of the 3%/3mm criterion was > 98% for three systems, the corresponding 3%/2mm and 2%/2mm criteria were > 95% and 90%. The average γ_{mean} of the three dose verification methods were 0.35, 0.38, 0.35 for the 3%/3mm criterion. Mans et al.[17] concluded that the overall quality of the EPID dose distribution was reflected in the γ parameters: γ_{mean}=0.39 and more than 97% of the volume fulfill γ≤1. Again, the SD of γ passing rates of the 3%/3mm criterion were 1.69%, 1.61%, 1.37% for EDose, Seven29, 3Dmap severally, which showed stability response obtained using the EDose system and consistent with the other two methods. All these results demonstrate the feasibility of the EDose system for pre-treatment dose verification.

In the study, three pre-treatment dose verification methods provide some advantages, such as overall accuracy compared with a single ionization chamber, besides convenience, accuracy, "real-time" reading compared with the film and thermoluminescent detectors measurements for the verification of IMRT/RapidArc plans.[] The near-water-equivalent plastic scintillators and synthetic diamond detectors can be used for many measurements of dosimetric quantities such as percent depth doses, tissue-phantom ratios, and beam profiles.[,] However, their relatively high cost may limit their use in many radiotherapy clinics. The amorphous silicon system EDose and 3Dmap provide a high spatial resolution compared to most other available dosimeters, vastly superior to the 2D array Seven29, and also superior to patient computed tomography datasets where voxel sizes are about 1×1×2mm^3.

The widely used 3% dose difference and 3mm distance-to-agreement criteria were introduced for comparing the measured and planned dose distributions in a single IMRT beam. Dose deviations in a single beam or segment will be diluted in the total dose distribution. Furthermore, Mans et al.[17] report that in vivo verification of the prostate plan shows slightly higher γ values

than pre-treatment. Wendling et al.[] propose the identical passing criteria always yields smaller γ values in 3D dose verification than in 2D. Therefore, the stricter γ criteria 3%/2mm and 2%/ 2mm were considered in the study.

The action level for patient QA had been established according to the γ index. Kim et al.[] suggested that the tolerance levels for IMRT delivery quality assurance (DQA) measurements using confidence limits determined by a multi-institutional study were established on 87.9% at 3%/3 mm using the composite film measurements. Chong et al.[] demonstrated how to perform and define appropriate action levels for the IMRT DQA using a 2D array diode detector MapCheck™, and reported the DQA passing rate action levels was 90%. Based on the ion chamber, as well as film measurements, Wen and Chung et al.[,] also had established institutional CLs values to ensure the high precision of IMRT delivery. Corresponding, our institutional CL value was 93% at the γ passing standard 3%/3mm according to the EDose measurements.

As radiotherapy becomes more and more complicated, tighter margins, and higher dose. Also, over a series of fractions, anatomical changes such as weight loss, flexing of the neck, and variation in lung density will result in dose delivery variation. [] Therefore, the real in vivo dosimetry will become necessary. 3D online dose verification means the images are acquired during treatment time, as for the routine use of portal imaging for patient set-up verification, which is a fast and direct procedure compared to pre-treatment verification. Additionally, the study results show that the EDose system can provide more detailed information, not only the gamma passing rate but also the preferable dose-volume histogram for the target volume and OARs, which ease the process of interpretation of possible differences and get a quick idea of the treatment plan.

Conclusion

The dosimetric characteristics study has shown that the EDose system implemented clinically in our department provided stable and consistent measurement outcomes and is a useful tool for the quality assurance of radiotherapy plans (pre-treatment as well as 3D online). The γ analysis between planned calculatation and EDose measurement dose distributions demonstrate excellent results for pre-treatment verification of 50 IMRT/RapidArc plans, as well as for 3D online verification of 28 radiotherapy plans. EDose is comparable to other commercialized systems (Seven29 and 3Dmap) used for similar pre-treatment radiotherapy delivery validation QA. The clinical action level was established at 92% with a 95% confidence limit using the institutional EDose measurements based on the 287 patients' pre-treatment verification data.

Declarations

Funding:

This study was funded by 1. Chongqing Science and Technology Commission (CSTC) (grant number cstc2019jscx-msxmX0265).

2. Science and Technology Innovation Ability Enhancement Special Project of Army Military Medical University (grant number 2019XLC3036).

Conflict of Interest:

Author xiaojuan duan declares that she has no conflict of interest. Author hongya dai declares that she has no conflict of interest. Author yibing zhou declares that she has no conflict of interest.

Ethical approval:

All procedures performed in studies involving human participants were in accordance with the ethical standards of the institutional and/or national research committee and with the 1964 Helsinki declaration and its later amendments or

comparable ethical standards.

Informed consent:

Informed consent was obtained from all individual participants included in the study.

References

1. Mijnheer B, Karellas A, Thomadsen BR, et al. Clinical 3D Dosimetry in Modern Radiation Therapy. New York: CRC Press, Taylor & Francis, 2017.
2. Li JS, Lin T, Chen LL, et al. Uncertainties in IMRT dosimetry. Medical Physics. 2010, 37(6): 2491-2500.
3. Buonamici FB, Compagnucci A, Marrazzo L, et al. An Intercomparison between Film Dosimetry and Diode Matrix for IMRT Quality Assurance. Medical Physics. 2007, 34(4), 1372-1379.
4. Kapulsky A, Gejerman G, Hanley J. A clinical application of an automated phantom-fifilm QA procedure for validation of IMRT treatment planning and delivery. Medical Dosimetry. 2004, 29(4): 279–284.
5. Lechner W, Primeßnig A, Nenoff L, et al. The influence of errors in small field dosimetry on the dosimetric accuracy of treatment plans. Acta Oncologica. 2020, 59(5): 511-517.
6. Markovic M, Narayanasamy G, Stathakis S, et al. Clinical Evaluation of a Two-dimensional Liquid-Filled Ion chamber Detector Array for Verification of High Modulation Small Fields in Radiotherapy. Journal of Medical Physics. 2019, 44(2): 91-98.
7. Stelljes TS, Poppinga D, Kretschmer J, et al. Experimental determination of the "collimator monitoring fill factor" and its relation to the error detection capabilities of various 2D-arrays. Medical Physics. 2019, 46(4): 1863-1873.
8. Valderrama AT, Olaciregui-Ruiz I, González PJ, et al. Portal Dosimetry of Small Unflattened Beams. Physics in Medicine & Biology. 2020. DOI: 10.1088/1361-6560/ab843d.
9. Arjunan M, Sekaran SC, Sarker B, et al. Electronic Portal Imaging Device-Based Three-Dimensional Volumetric Dosimetry for Intensity-modulated Radiotherapy Pretreatment Quality Assurance. Journal of Medical Physics. 2019, 44(3): 176-184.
10. McCurdy BMC, McCowan PM. In vivo dosimetry for lung radiotherapy including SBRT. Physica Medica. 2017, 44, 123-130.
11. Hashemi SM, Bahreyni MH, Mohammadi M, et al. An Empirical Transmitted EPID Dosimetry Method using a Back-Projection Algorithm. Journal of Biomedical Physics Engineering. 2019, 9(5): 551-558.
12. Najem MA, Tedder M, King D, et al. In-vivo EPID dosimetry for IMRT and VMAT based on through-air predicted portal dose algorithm. Physica Medica. 2018, 52: 143-153.
13. Gandhi A, Vellaiyan S, Subramanian VS, et al. Commissioning of portal dosimetry using a novel method for flattening filter-free photon beam in a nontrue beam linear accelerator. Journal of Cancer Research and Therapeutics. 2019, 15(1): 223-230.
14. Zhu J, Chen L, Chen A, Luo G, Deng X, Liu X. Fast 3D dosimetric verifications based on an electronic portal imaging device using a GPU calculation engine. Radiat Oncol. 2015, 10:1-11.
15. Huang MY, Huang D, Zhang JP, et al. Preliminary study of clinical application on IMRT three-dimensional dose verification-based EPID system. Journal of Applied Clinical Medical Physics. 2017, 18(4): 97-105.
16. Low DA, Moran JM, Dempsey JF, et al. Dosimetry tools and techniques for IMRT. Med Phys, 2011, 38(3): 1313-1338.
17. Poppe B, Blechschmidt A, Djouguela A, et al. Two-dimensional ionization chamber arrays for IMRT plan verifification. Med Phys, 2006, 33(4): 1005-1015.
18. Ezzel GA, Burmeister JW, Dogan N, et al. IMRT Commissioning: Multiple Institutions Planning and Dosimetry Comparisons, a report from AAPM Task Group 119. Medical Physics. 2009, 36(11): 5359-5373.
19. Mans A, Remeijer P, Olaciregui-Ruiz I, et al. 3D Dosimetric verification of volumetric-modulated arc therapy by portal dosimetry. Radiotherapy and Oncology. 2010, 94(2): 181-187.

20. Bedford J L, Hanson IM, Hansen VN. Comparison of forward- and back-projection in vivo EPID dosimetry for VMAT treatment of the prostate. Physics in Medicine & Biology. 2018, 63(2): 025008.
21. Huang MY, Huang D, Zhang JP, et al. Preliminary study of clinical application on IMRT three-dimensional dose verification-based EPID system. Journal of Applied Clinical Medical Physics, 2017, 18(4), 97-105.
22. Esch AV, Huyskens DP, Hirschi L, et al. Optimized Varian aSi portal dosimetry: development of datasets for collective use. Journal of Applied Clinical Medical Physics. 2013, 14(6): 82-99.
23. Berry SL, Polvorosa CS, Wuu C-S. A field size specific backscatter correction algortihm for accurate EPID dosimetry. Med Phys. 2010,37(6): 2425-2434.
24. IAEA. Dosimetry of Small Static Fields Used in External Beam Radiotherapy: An IAEA-AAPM International Code of Practice for Reference and Relative Dose Determination. Technical Reports Series No. 483. 2017. (Vienna, Austria: International Atomic Energy Agency, IAEA).
25. Das IJ, Ding GX and Ahnesjo A. Small fields: Non-equilibrium radiation dosimetry. Med. Phys. 2008, 35: 206-215.
26. Syamkumar SA, Padmanabhan S, Sukumar P, et al. Characterization of responses of 2d array seven29 detector and its combined use with octavius phantom for the patient-specific quality assurance in rapidarc treatment delivery. Medical Dosimetry, 2012, 37(1): 53-60.
27. Therriault-Proulx F, Pino R, Yang JN, et al. Quality assurance for gamma knife perfexion using the exradin W1 plastic scintillation detector and Lucy phantom. Physics in Medicine and Biology. 2019, 64(22): 225007.
28. Russo S, Masi L, Francescon P, et al. Multicenter evaluation of a synthetic single-crystal diamond detector for CyberKnife small field size output factors. Physica Medica, 2016, 32(4): 575-581.
29. Wendling M, Zijp LJ, McDermott LN, et al. A fast algorithm for gamma evaluation in 3D. Medical Physics, 2007, 34(5):1647-1654.
30. Kim JI, Chung JB, Park YK, et al. A multi-institutional study for tolerance and action levels of IMRT dose quality assurance measurements in Korea. Journal of Applied Clinical Medical Physics, 2013, 14(2): 24-37.
31. Chong NS, Lee JJS, Kung W-H, et al. Patient Delivery Quality Assurance for Linac-Based IMRT and Helical Tomotherapy Using Solid State Detectors. Radiation Measurements, 2011, 46(12): 1993-1995.
32. Wen N, Zhao B, Kim J, et al. IMRT and RapidArc commissioning of a TrueBeam linear accelerator using TG-119 protocol cases. Journal of Applied Clinical Medical Physics, 2014, 15(5): 74-88.
33. Chung JB, Kim JS, Ha SW, et al. Statistical analysis of IMRT dosimetry quality assurance measurements for local delivery guideline. Radiation Oncology, 2011, 6(1): 27.
34. Van Elmpt W, McDermott L, Nijsten S, et al. A literature review of electronic portal imaging for radiotherapy dosimetry. Radiotherapy and Oncology, 2008, 88(3): 289-309.

Figures

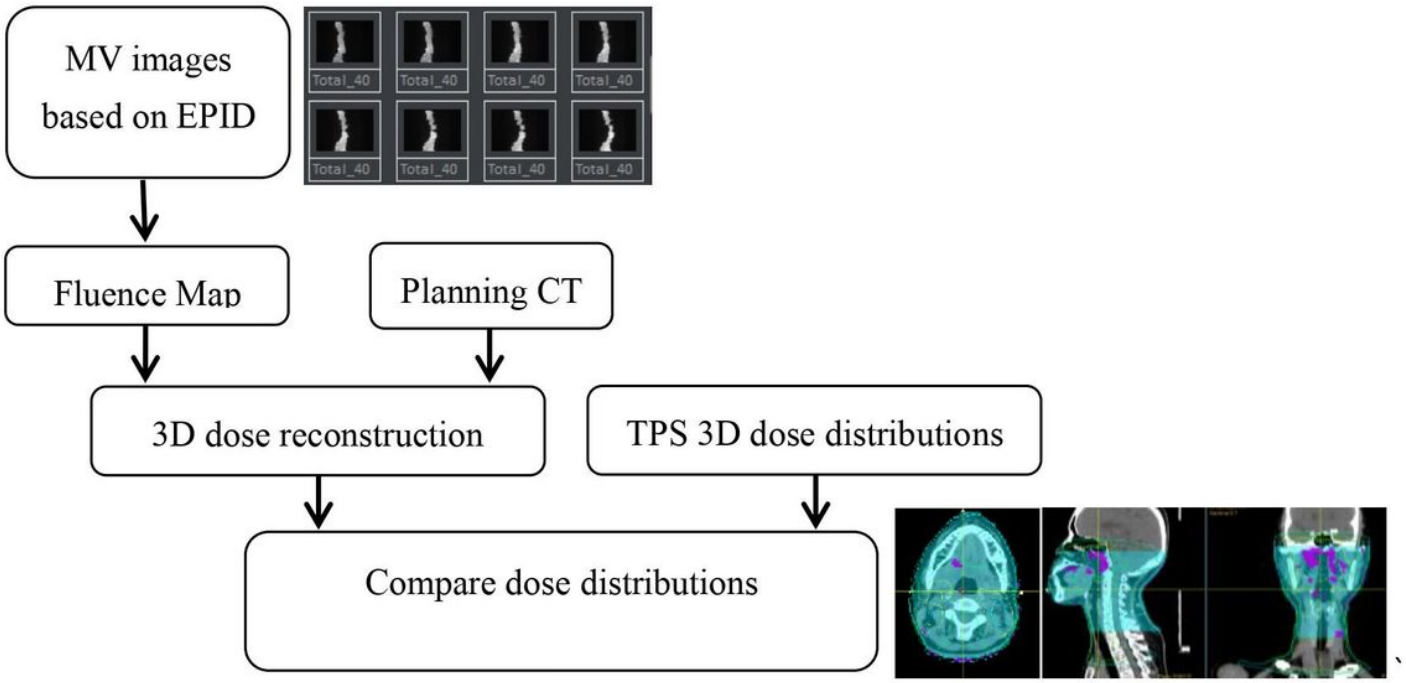

Figure 1

The workflow of EDose system dose verification

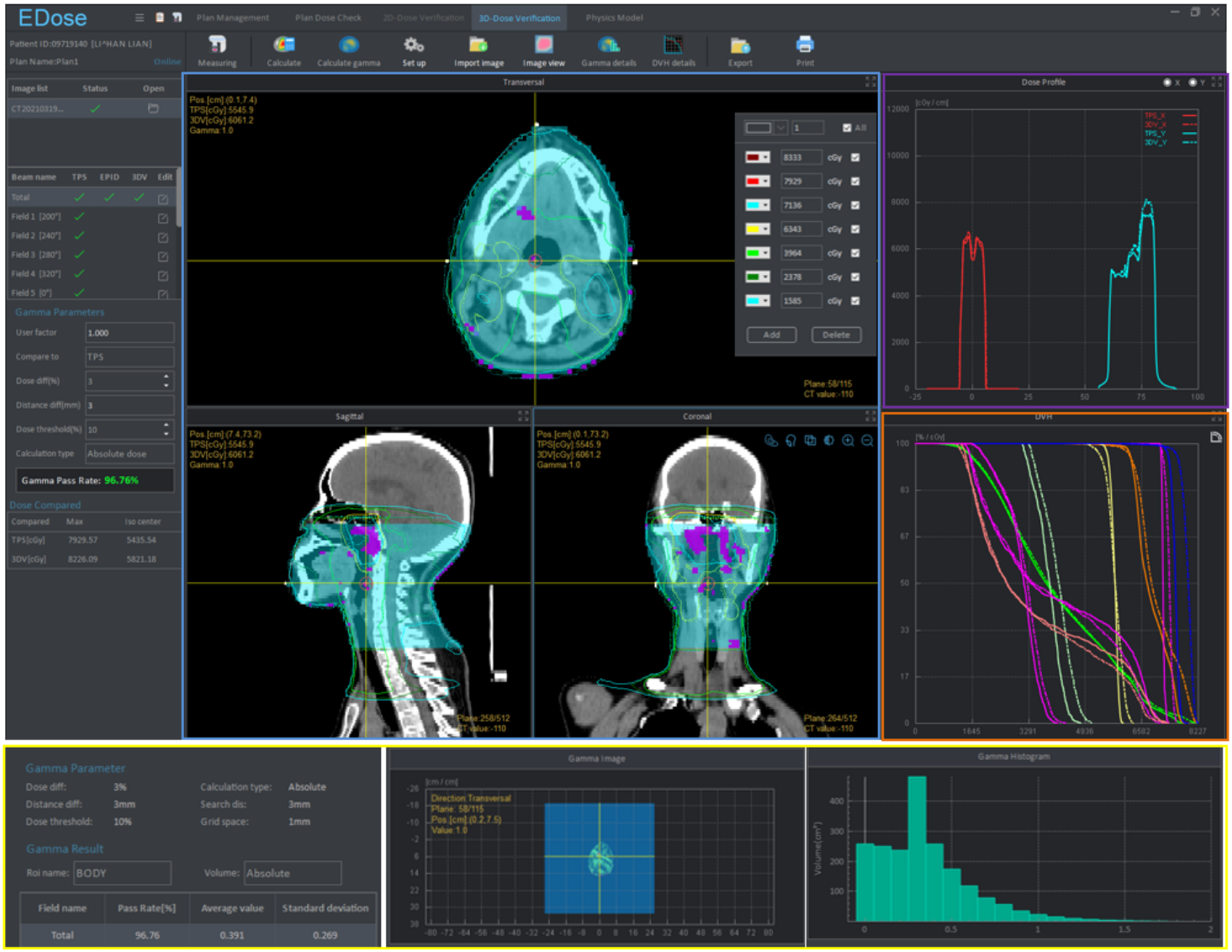

Figure 2

Evaluation tools of the EDose system

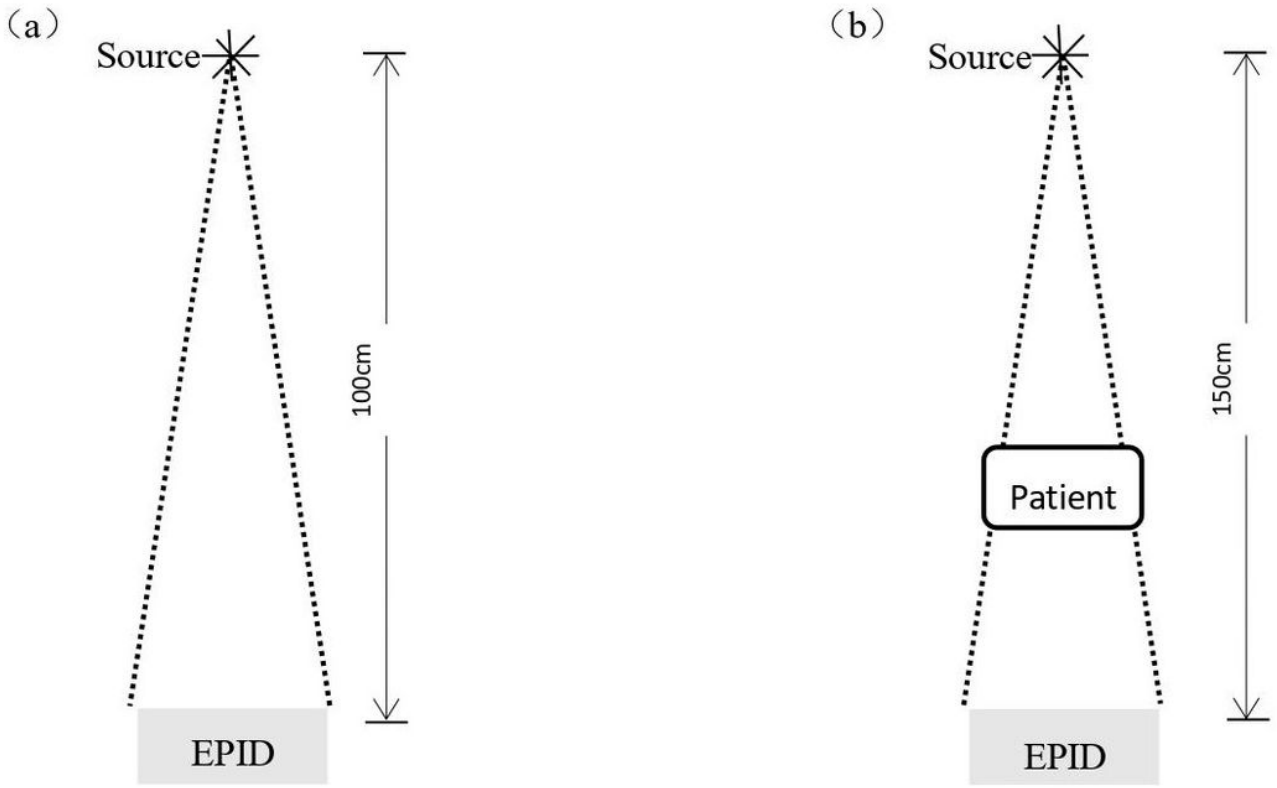

Figure 3

Schematic diagram for the position of EPID. (a) pre-treatment verification: EPID detectors was positioned at the isocenter with a distance 100cm and non-transmission; (b) 3D online dose verification: EPID detectors was positioned at the distance 150cm and with patient transmission.

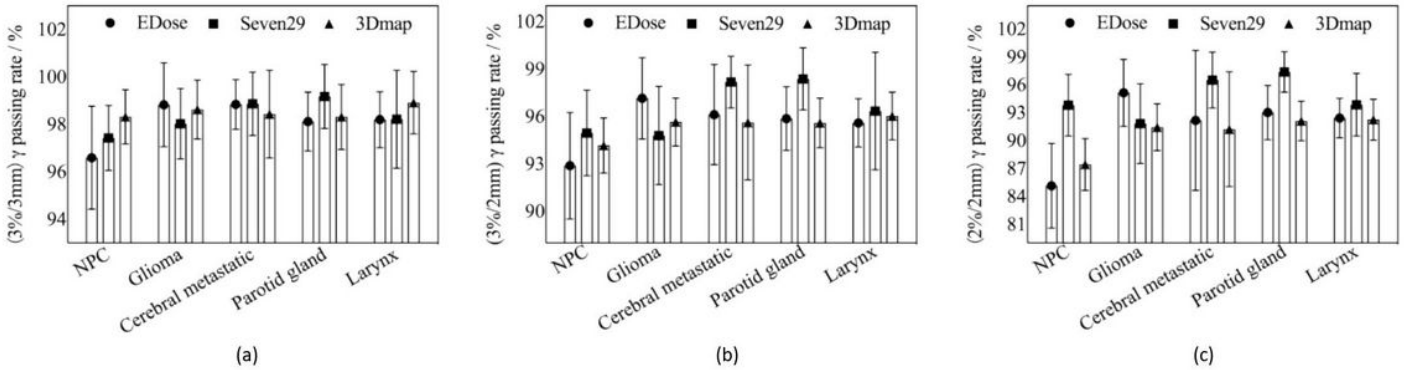

Figure 4

γ passing rates for the 5 kinds of disease obtained from EDose, Seven29 and 3Dmap measurements respectively. (a) 3%/3mm criteria; (b) 3%/2mm criteria; (c) 2%/2mm criteria; The columns represent the mean values of the γ passing rates, and the error bars are the corresponding SD.

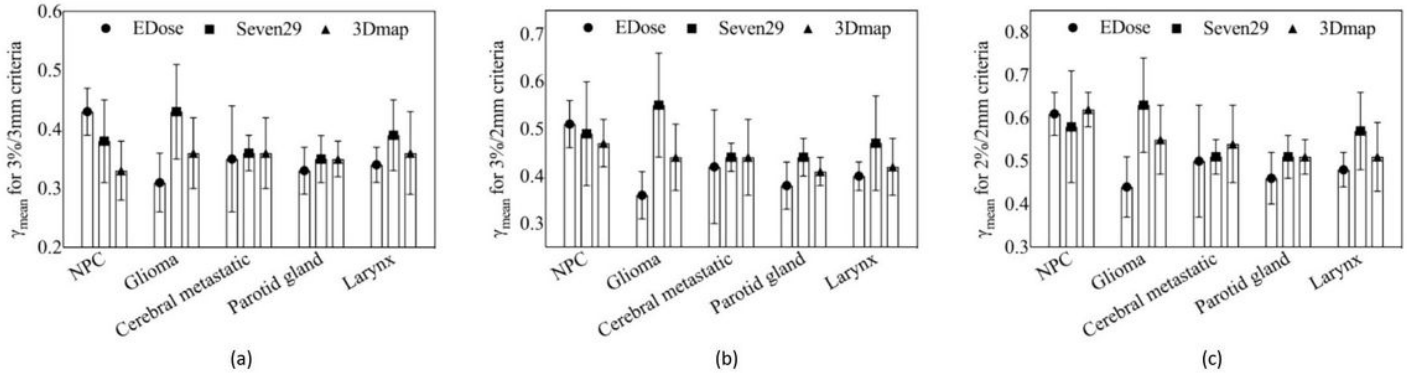

Figure 5

γmean for the 5 kinds of disease obtained from EDose, Seven29 and 3Dmap measurements respectively. (a) 3%/3mm criteria; (b) 3%/2mm criteria; (c) 2%/2mm criteria; The columns represent the mean values of the γmean and the error bars are the corresponding SD.

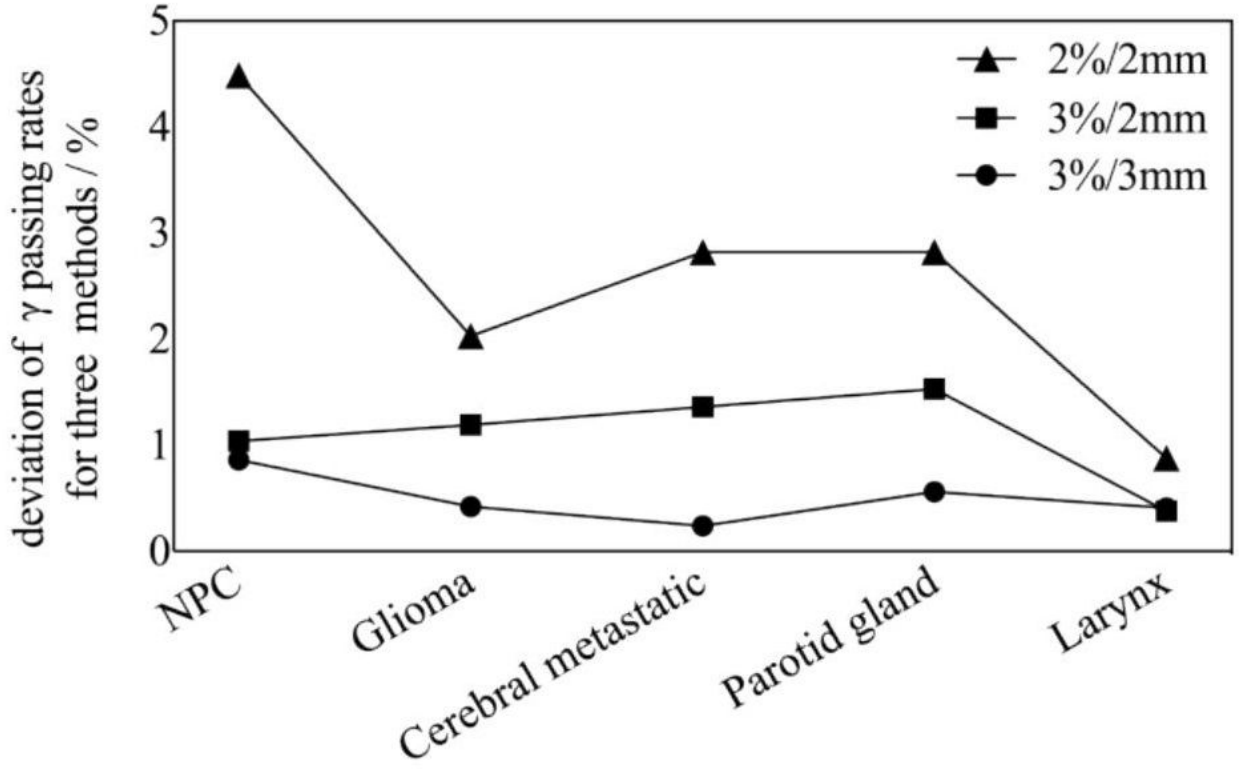

Figure 6

Deviation of γ passing rates for three dose verification methods.

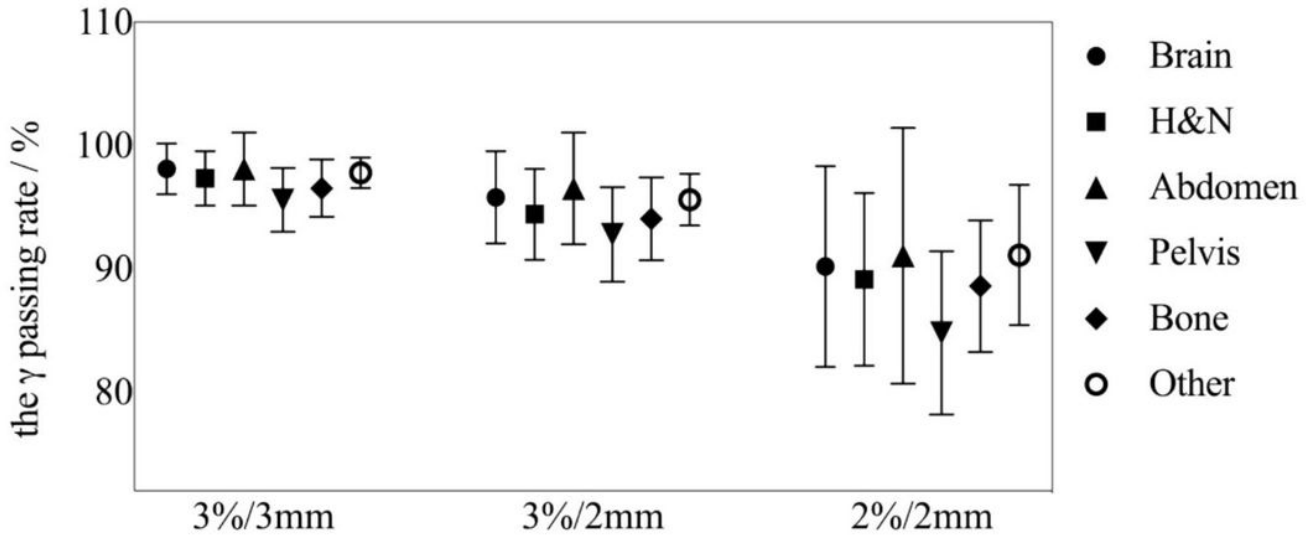

Figure 7

Comparison of the average γ passing rates for the 287 IMRT/RapidArc cases obtained from EDose measurements in different disease sites under three criteria 3%/3mm, 3%/2mm, and 2%/2mm respectively. Error bars represent the SD of the corresponding γ passing rates.

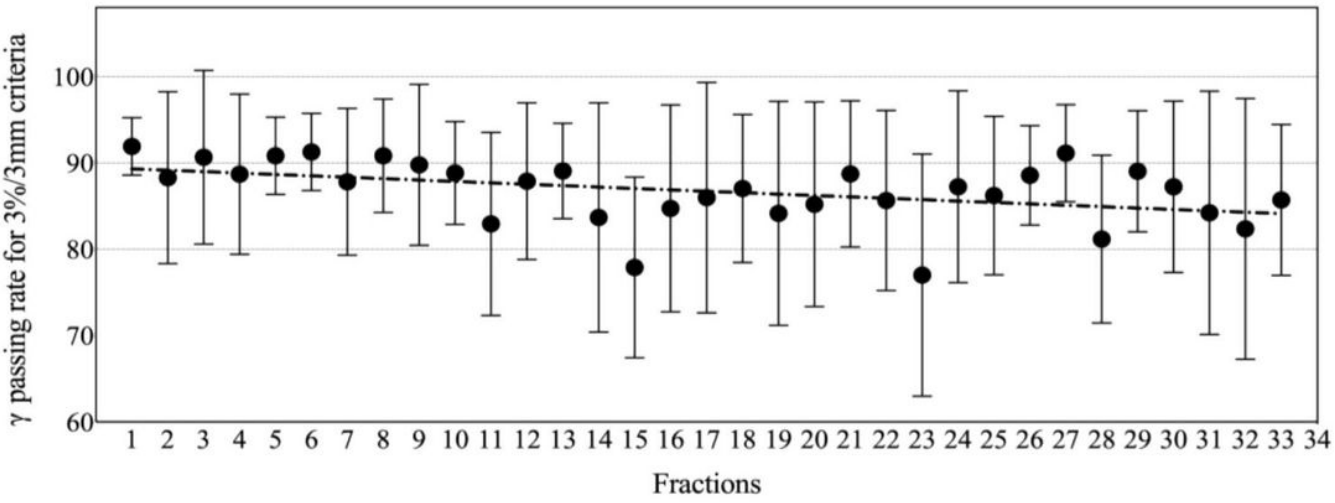

Figure 8

Results of 33 fractions in vivo dose monitoring in 28 patients. The dot line was the result of linear regression of the average γ pass rate.

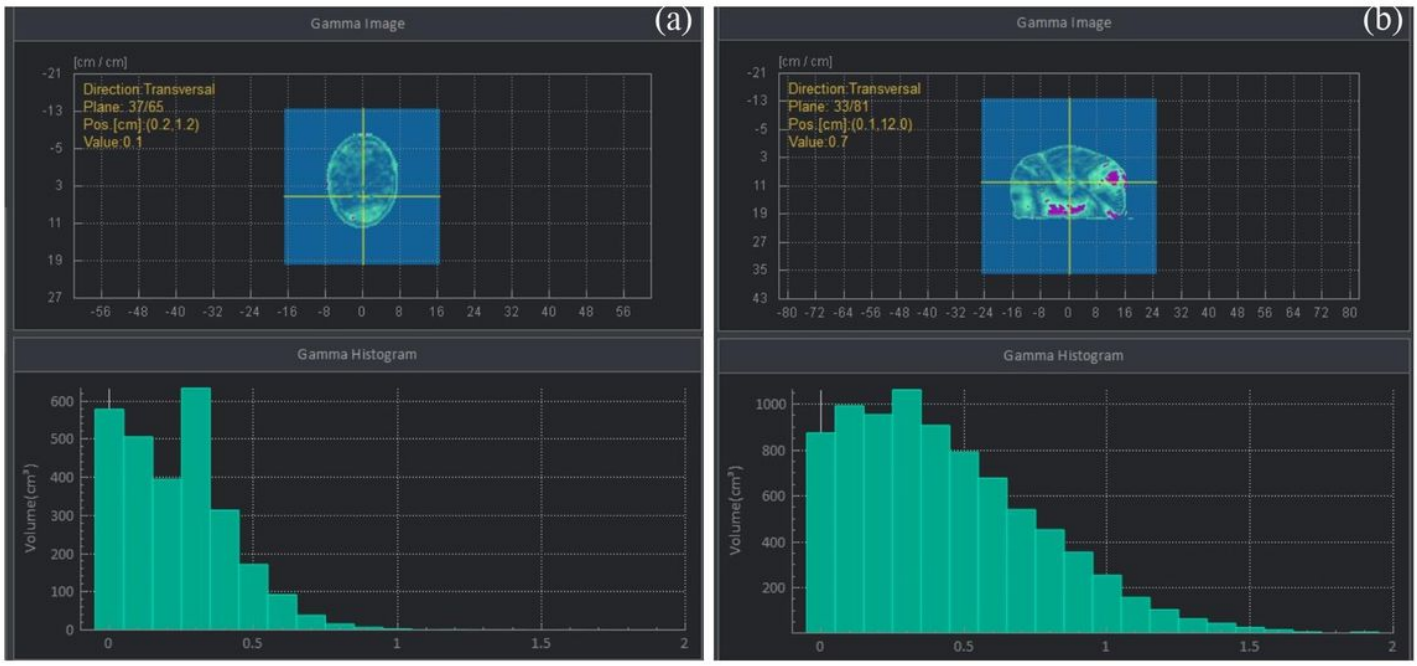

Figure 9

Gamma image distributions in transversal view and Gamma histogram using EDose 3D online dose verification under the 3%/3 mm criterion. (a) a brain metastasis patient with a γ passing rate of 99.84%. (b) a rectal cancer patient with a γ passing rate of 91.70%. The green represents the passing region, while the pink region represents the failure to pass in the Gamma image.

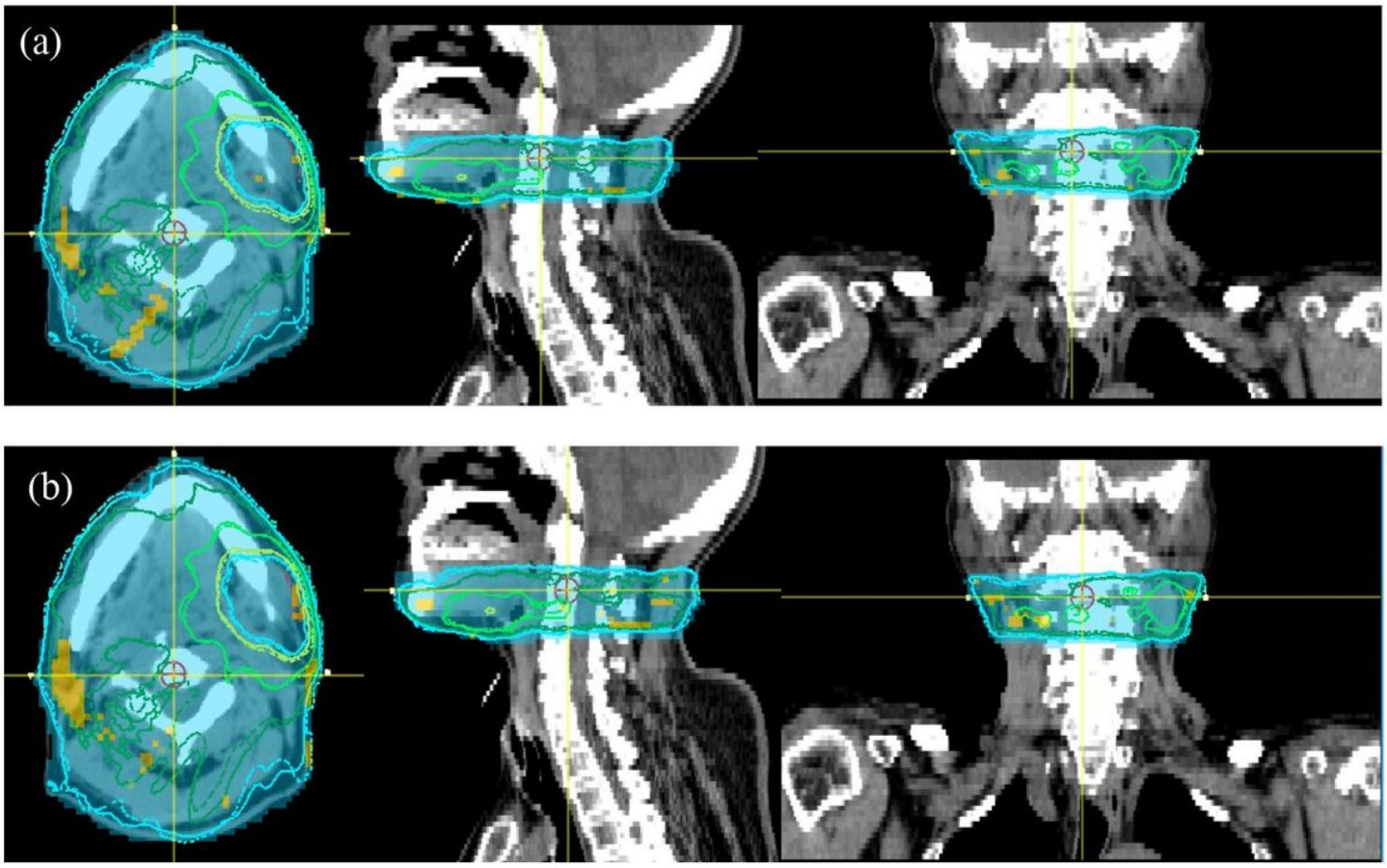

Figure 10

Gamma image distributions in isocentric plane of a patient with cervical lymph node metastases. (a) 3D online dose verification with a passing rate 97.06%; (b) pre-treatment dose verification with a passing rate 95.60%. The sky blue represents the passing region, while the yellow area represents the the failed region.